Optical field emission from resonant gold nanorods driven by femtosecond mid-infrared pulses

F. Kusa,[1,2,a] K. E. Echternkamp,[3,a] G. Herink,[3] C. Ropers,[3] and S. Ashihara[2,b]
[1]*Department of Applied Physics, Tokyo University of Agriculture and Technology, 2-24-16 Nakacho, Koganei Tokyo 184-8588, Japan*
[2]*Institute of Industrial Science, the University of Tokyo, 4-6-1 Komaba, Meguro-ku, Tokyo 153-8505, Japan*
[3]*4th Physical Institute – Solids and Nanostructures, University of Göttingen, 37077 Göttingen, Germany*

(Received 25 April 2015; accepted 9 July 2015; published online 16 July 2015)

We demonstrate strong-field photoelectron emission from gold nanorods driven by femtosecond mid-infrared optical pulses. The maximum photoelectron yield is reached at the localized surface plasmon resonance, indicating that the photoemission is governed by the resonantly-enhanced optical near-field. The wavelength- and field-dependent photoemission yield allows for a noninvasive determination of local field enhancements, and we obtain intensity enhancement factors close to 1300, in good agreement with finite-difference time domain computations. [http://dx.doi.org/10.1063/1.4927151]

Over the past years, strong-field light-matter interaction has increasingly been studied at surfaces and nanostructures, featuring local field enhancements and sub-wavelength confinement of optical near-fields. Nonlinear photoelectron emission, a prominent phenomenon in this area, has been intensively studied for various individual metallic nanostructures,[1–9] thin films[10,11] or antenna arrays,[12–15] with motivations for optically-controlled electron propagation in ultrafast electronics,[16] ultrafast electron[17–19] and x-ray sources,[20] as well as phase-resolved imaging and spectroscopy.[16,21]

Metal nanotips displaying broadband near-field enhancements present a prominent model system for highly nonlinear photoelectron emission and acceleration, and studies have been conducted in the visible to near-infrared,[1,3,7,22,23] mid-infrared[6] and Terahertz ranges[16,24] Nanoparticles and plasmonic antennas constitute another platform for photoemission studies,[8,9,15,25] as they exhibit field enhancements from resonant surface plasmon modes,[25–27] which may be further amplified by geometric edge enhancements. Recent work has investigated resonance-enhanced nonlinear photoemission at near-infrared frequencies.[9,12]

Resonant nanostructures in the mid-infrared (MIR) spectral range offer attractive features in photoemission, yielding access to the strong-field regime at reduced local intensities,[6,11] and providing for higher ponderomotive energies as well as novel sub-cycle regimes in photoelectron acceleration.[6] Furthermore, low absorption and reduced radiative damping lead to increased damage thresholds and larger field enhancements,[28,29] respectively.

In this Letter, we study strong-field photoemission from resonant gold nanorods driven by femtosecond MIR pulses. The wavelength-dependent, nonlinear photoelectron yield follows the resonance profile of the nanorods, and intensity-dependent measurements allow for a noninvasive determination of the local intensity (field) enhancement factors, reaching 1290 (36) at the resonance. This quantitative information on the enhancement factor, which cannot be obtained from far-field characterization alone, is of immediate relevance for plasmon-assisted spectroscopy, such as surface-enhanced infrared absorption spectroscopy.[30–32]

[a]These authors contributed equally to this work.
[b]Corresponding author: ashihara@iis.u-tokyo.ac.jp

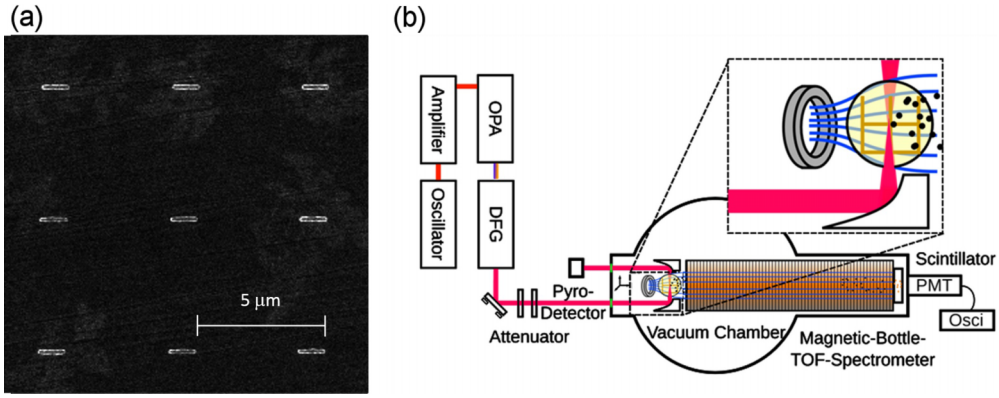

FIG. 1. (a) Scanning electron micrograph of a nanorod array (rod length 1 µm). (b) Experimental setup. Tunable mid-infrared pulses are focused onto a nanorod array in a high vacuum chamber. Electron kinetic energy spectra are measured with a magnetic-bottle time-of-flight spectrometer.

For the experiments, two-dimensional arrays (1100 × 1100 elements) of gold nanorods (length: 1 µm, width: 150 nm, height: 50 nm) are fabricated on ZnS substrates (zinc blende structure) with a Cr adhesion layer by electron beam lithography and a lift-off process (Fig. 1(a)). A spacing of 5 µm between the rods prevents possible near-field couplings.[33–35] A 5-nm-thick gold capping serves as a conduction layer to avoid sample charge-up during photoemission.

MIR pulses at center wavelengths tunable from 3-10 µm and pulse durations of about 160 fs are produced by difference frequency generation (DFG) of signal and idler waves from an optical parametric amplifier (OPA), pumped by amplified Ti:Sapphire laser pulses (central wavelength: 800 nm, pulse duration: 50 fs, repetition rate: 1 kHz). A parabolic mirror (see Fig. 1(b)) is used to focus the MIR pulses at near normal incidence to spot diameters of about 30 µm. In order to illuminate multiple rods (typically around 8000) and to minimize the influence of chromatic variations in focusing, the sample was placed at a defocus position with a beam diameter of about 500 µm, giving rise to incident peak intensities of 0.5-1.5 GW/cm^2 for pulse energies of 80-230 nJ and pulse durations measured as a function of wavelength. For a polarization parallel to the nanorod axis, we excite a fundamental longitudinal mode (the half-wave dipole antenna mode) with a resonance wavelength of 5 µm. Photoelectrons emitted from the nanostructures are guided by a magnetic-bottle to a time-of-flight (TOF) spectrometer for measurements of the photoelectron yields and kinetic energy spectra.[36]

Figure 2(a) displays the photoelectron yields as a function of incident peak intensity for different excitation wavelengths on a double-logarithmic scale. All curves exhibit a strongly nonlinear intensity-dependence and shift to lower intensity for excitation wavelengths closer to the resonance, which illustrates the underlying near-field enhancement.

To characterize the photoemission regime and for an evaluation of the local field enhancement, the intensity-dependence of the electron yield is analyzed by fitting the Fowler-Nordheim (FN) equation to the data, including barrier reduction (Schottky effect),[37] as shown in Fig. 2 (solid lines), e.g., in Fig. 2(b) for 5.0 µm excitation. In fitting the yields, we use the work function of 5.1 eV for polycrystalline gold.[38,39] Throughout the measured intensity range, the nonlinearity of the yield decreases with intensity (the local slope varies from ~9 to ~7 in the peak intensity range of 0.65-1.3 GWcm^{-2}) and remains smaller than a corresponding multi-photon dependence (slope 20 at a photon energy of 0.25 eV and the 5.1 eV work function). From the FN fits, we deduce a local electric-field amplitude of 3.5 Vnm^{-1} and a Keldysh parameter[40] $\gamma = \sqrt{\phi/2U_p}$ of approximately 0.80, which indicates optical field emission as the underlying process (metal work function ϕ, ponderomotive energy $U_p = e^2E^2/4m\omega^2$, with e, m the electron charge and mass, respectively, E the electric-field amplitude and ω the optical frequency). It should be noted that the total experimental electron yield per antenna is significantly reduced compared to both theoretical expectations and measurements at single nanotips. This is caused by the low collection efficiency in the magnetic bottle geometry in conjunction with a surface and the resulting high fraction of electrons reabsorbed

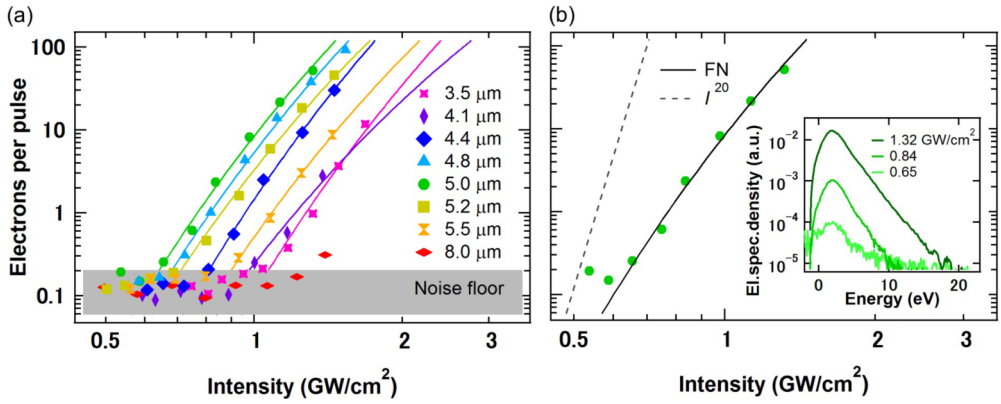

FIG. 2. (a) Electron yield for different excitation wavelengths as a function of incident intensity. Each curve is fitted by Fowler-Nordheim equation (solid line) to extract the intensity enhancement factor. (b) Fowler-Nordheim fit to the electron yield at 5 μm wavelength (solid line). For comparison, a corresponding multiphoton dependence (dashed line, slope 20) is shown. Inset: Electron kinetic energy spectra for selected intensities.

by the substrate. To reduce the influence of an energy-dependent detection yield, we applied a static bias voltage of 10 V to the surface. The inset in Fig. 2(b) shows kinetic energy spectra of photoelectrons for several incident intensities at 5 μm excitation (static bias potential subtracted). The kinetic energy cutoff (when defined to include 99% of the electron population) is found to linearly increase with intensity, consistent with a ponderomotive scaling.[41]

The measured far-field extinction spectrum of the nanorod array, shown in Fig. 3(a), exhibits a resonance at a wavelength of 5 μm. Figure 3(b) displays the photoelectron yield for a range of excitation wavelengths at a constant incident intensity of 1.1 GW/cm^2 (triangles). The photoelectron yield also sharply peaks around 5 μm, confirming that the nonlinear photoemission process is governed by the resonantly enhanced near-field. The intensity enhancement factor obtained from the FN fits to the electron yield curves (Fig. 2(a)) is plotted as circles in Fig. 3(b), and we find a maximum intensity (field) enhancement value of 1290 (36). The photoelectron yield exhibits a

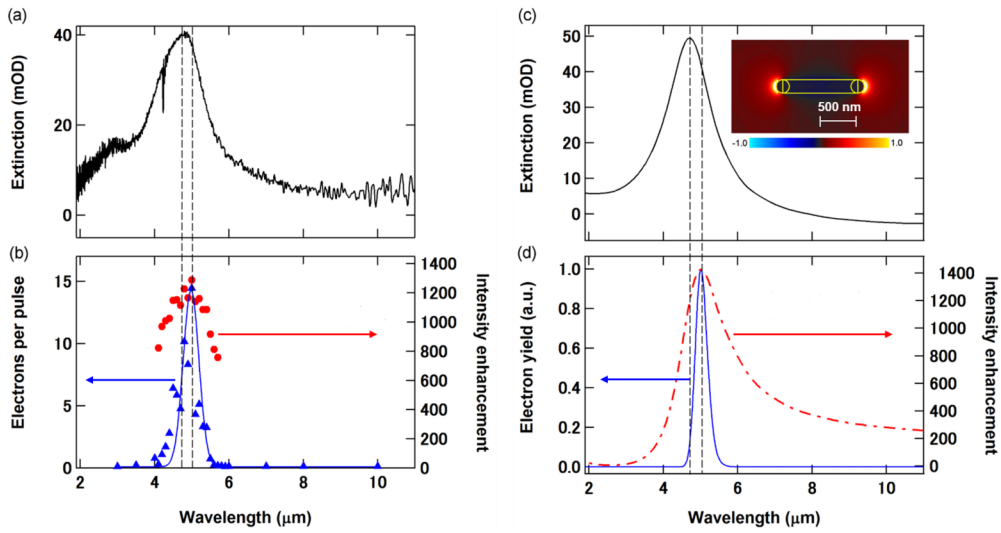

FIG. 3. (a) Measured far-field extinction spectrum. (b) Triangles: Experimental photoemission yield as a function of excitation wavelength and for constant incident intensity. Circles: Intensity enhancement factors extracted from the corresponding yield curves. (c) Simulated far-field extinction spectrum for $L = 1$ μm nanorods. Inset: Normalized electric field component parallel to the nanorod. Wavelength: 5 μm. (d) Simulated local intensity enhancement factor (dashed-dotted line) and electron yield (solid line) as a function of the excitation wavelength. Dashed vertical lines indicate red-shift of spectral near-field enhancement relative to far-field extinction spectrum in both experiment (a,b) and simulation (c,d).

much sharper resonance profile than the underlying optical near-field due to the high nonlinearity of the emission process. In the determination of the intensity enhancement from the nonlinear photoemission yield, some uncertainties arise: A finite uncertainty in the incident peak intensity may lead to an error up to 13% in the intensity enhancement, and local variations in the work function may also influence the values determined For example, using the 5.47 eV work function of the low index plane of gold-(100) in fitting the yield curves results in an intensity enhancement value of ~1580.

To support our experimental results, we performed numerical simulations of the electromagnetic field distribution with the 3D-FDTD method.[29] The nanorods are modeled with the experimental dimensions (length: 1 μm, height: 50 nm, width: 150 nm) using a rectangular cross-section and two half-cylinders at both ends (see inset of Fig. 3(c)). The simulated far-field extinction (Fig. 3(c)) is in good agreement with the experiments, exhibiting an asymmetric resonance around 5 μm with a linewidth of 21 THz. The inset in Fig. 3(c) shows the spatial distribution of the electric-field component parallel to the nanorod axis (5 μm excitation). The wavelength-dependent intensity enhancement at the position of the largest electric field is shown as a dashed-dotted line in Fig. 3(d), and the maximum value of approximately 1400 agrees well with the experiment. Using the FN equation, the solid line represents the expected photoelectron yield, which reduces the width of the line profile to 5 THz (experimental width: ~6 THz). In both the experiment and the simulations, the near-field enhancement is highest at a slightly red-shifted wavelength (experiment: 0.2 μm, simulation: 0.3 μm) compared to the far-field extinction spectrum (see vertical dashed lines in Figs. 3(a), 3(b) and 3(c), 3(d)). Such spectral shifts between near- and far-field spectra are universal to damped harmonic oscillators[42] and were previously observed in scanning near-field optical microscopy.[43] In this respect, the nonlinear photoemission process exhibits some advantages in being an intrinsically noninvasive local probe.

In conclusion, we demonstrate resonance-enhanced strong-field photoelectron emission from gold nanorods driven by femtosecond MIR pulses. Intensity-dependent measurements allow for a quantitative determination of the local field enhancement and its spectrum, and excellent agreement with numerical simulations is found. The results demonstrate the suitability of nonlinear photoemission in precise near-field characterizations, and may be generalized to other structures and geometries, including coupled nanostructures and high-density arrays.

ACKNOWLEDGMENT

Financial support by the Japan Society for the Promotion of Science (MEXT KAKENHI 26600113) and the Deutsche Forschungsgemeinschaft (SPP 1391 "Ultrafast Nanooptics" and SFB 1073, project A05) is gratefully acknowledged. The gold nanorods have been fabricated at VLSI Design and Education Center (VDEC), the University of Tokyo.

[1] P. Hommelhoff, Y. Sortais, A. Aghajani-Talesh, and M. A. Kasevich, Phys. Rev. Lett. **96**, 077401 (2006).
[2] C. Ropers, D. R. Solli, C. P. Schulz, C. Lienau, and T. Elsaesser, Phys. Rev. Lett. **98**, 043907 (2007).
[3] R. Bormann, M. Gulde, A. Weismann, S. V. Yalunin, and C. Ropers, Phys. Rev. Lett. **105**, 147601 (2010).
[4] M. Schenk, M. Kruger, and P. Hommelhoff, Phys. Rev. Lett. **105**, 257601 (2010).
[5] M. Kruger, M. Schenk, and P. Hommelhoff, Nature **475**, 78 (2011).
[6] G. Herink, D. R. Solli, M. Gulde, and C. Ropers, Nature **483**, 190 (2012).
[7] M. R. Bionta, B. Chalopin, J. P. Champeaux, S. Faure, A. Masseboeuf, P. Moretto-Capelle, and B. Chatel, J. Mod. Optic. **61**, 833 (2014).
[8] V. Schweikhard, A. Grubisic, T. A. Baker, and D. J. Nesbitt, J. Phys. Chem. C **115**, 83 (2011).
[9] A. Grubisic, V. Schweikhard, T. A. Baker, and D. J. Nesbitt, Acs Nano **7**, 87 (2013).
[10] P. Dombi, S. E. Irvine, P. Racz, M. Lenner, N. Kroo, G. Farkas, A. Mitrofanov, A. Baltuska, T. Fuji, F. Krausz, and A. Y. Elezzabi, Opt. Express **18**, 24206 (2010).
[11] S. M. Teichmann, P. Racz, M. F. Ciappina, J. A. Perez-Hernandez, A. Thai, J. Fekete, A. Y. Elezzabi, L. Veisz, J. Biegert, and P. Dombi, Sci. Rep. **5**, 7584 (2015).
[12] P. Dombi, A. Horl, P. Racz, I. Marton, A. Trugler, J. R. Krenn, and U. Hohenester, Nano Lett. **13**, 674 (2013).
[13] P. M. Nagel, J. S. Robinson, B. D. Harteneck, T. Pfeifer, M. J. Abel, J. S. Prell, D. M. Neumark, R. A. Kaindl, and S. R. Leone, Chem. Phys. **414**, 106 (2013).
[14] P. D. Keathley, A. Sell, W. P. Putnam, S. Guerrera, L. Velasquez-Garcia, and F. X. Kartner, Ann. Phys. **525**, 144 (2013).
[15] R. G. Hobbs, Y. Yang, A. Fallahi, P. D. Keathley, E. De Leo, F. X. Kartner, W. S. Graves, and K. K. Berggren, Acs Nano **8**, 11474 (2014).
[16] L. Wimmer, G. Herink, D. R. Solli, S. V. Yalunin, K. E. Echternkamp, and C. Ropers, Nat. Phys. **10**, 432 (2014).
[17] M. Gulde, S. Schweda, G. Storeck, M. Maiti, H. K. Yu, A. M. Wodtke, S. Schafer, and C. Ropers, Science **345**, 200 (2014).

[18] A. Mustonen, P. Beaud, E. Kirk, T. Feurer, and S. Tsujino, Appl. Phys. Lett. **99**, 103504 (2011).
[19] D. S. Yang, O. F. Mohammed, and A. H. Zewail, Proc. Natl. Acad. Sci. U. S. A. **107**, 14993 (2010).
[20] W. S. Graves, F. X. Kartner, D. E. Moncton, and P. Piot, Phys. Rev. Lett. **108**, 263904 (2012).
[21] M. I. Stockman, M. F. Kling, U. Kleineberg, and F. Krausz, Nature Photon. **1**, 539 (2007).
[22] H. Yanagisawa, M. Hengsberger, D. Leuenberger, M. Klockner, C. Hafner, T. Greber, and J. Osterwalder, Phys. Rev. Lett. **107**, 087601 (2011).
[23] D. J. Park, B. Piglosiewicz, S. Schmidt, H. Kollmann, M. Mascheck, and C. Lienau, Phys. Rev. Lett. **109**, 244803 (2012).
[24] G. Herink, L. Wimmer, and C. Ropers, New J .Phys. **16**, 123005 (2014).
[25] R. L. Olmon, P. M. Krenz, A. C. Jones, G. D. Boreman, and M. B. Raschke, Opt. Express **16**, 20295 (2008).
[26] M. Schnell, A. Garcia-Etxarri, A. J. Huber, K. Crozier, J. Aizpurua, and R. Hillenbrand, Nature Photon. **3**, 287 (2009).
[27] M. Eisele, T. L. Cocker, M. A. Huber, M. Plankl, L. Viti, D. Ercolani, L. Sorba, M. S. Vitiello, and R. Hober, Nature Photon. **8**, 841 (2014).
[28] F. Neubrech, D. Weber, R. Lovrincic, A. Pucci, M. Lopes, T. Toury, and M. L. de la Chapelle, Appl. Phys. Lett. **93**, 163105 (2008).
[29] F. Kusa and S. Ashihara, J. Appl. Phys. **116**, 153103 (2014).
[30] A. Pucci, F. Neubrech, D. Weber, S. Hong, T. Toury, and M. L. de la Chapelle, Phys. Status. Solidi. B **247**, 2071 (2010).
[31] L. V. Brown, K. Zhao, N. King, H. Sobhani, P. Nordlander, and N. J. Halas, J. Am. Chem. Soc. **135**, 3688 (2013).
[32] K. Chen, R. Adato, and H. Altug, Acs Nano **6**, 7998 (2012).
[33] N. Liu and H. Giessen, Angew. Chem. Int. Ed. **49**, 9838 (2010).
[34] D. Diessel, M. Decker, S. Linden, and M. Wegener, Opt. Lett. **35**, 3661 (2010).
[35] R. Taubert, R. Ameling, T. Weiss, A. Christ, and H. Giessen, Nano Lett. **11**, 4421 (2011).
[36] P. Kruit and F. H. Read, J. Phys. E **16**, 313 (1983).
[37] C. A. Spindt, I. Brodie, L. Humphrey, and E. R. Westerberg, J. Appl. Phys. **47**, 5248 (1976).
[38] H. B. Michaelson, J. Appl. Phys. **48**, 4729 (1977).
[39] W. N. Hansen and K. B. Johnson, Surf. Sci. **316**, 373 (1994).
[40] L. V. Keldysh, Sov. Phys. Jetp-Ussr. **20**, 1307 (1965).
[41] G. G. Paulus, W. Becker, and H. Walther, Phys Rev A **52**, 4043 (1995).
[42] J. Zuloaga and P. Nordlander, Nano Lett. **11**, 1280 (2011).
[43] P. Alonso-Gonzalez, P. Albella, F. Neubrech, C. Huck, J. Chen, F. Golmar, F. Casanova, L. E. Hueso, A. Pucci, J. Aizpurua, and R. Hillenbrand, Phys. Rev. Lett. **110**, 203902 (2013).